



1

2 **Long-term visibility variation in Athens (1931-2013): A proxy for local and regional**
3 **atmospheric aerosol loads**

4 Dimitra Founda¹, Stelios Kazadzis^{1,2}, Nikolaos Mihalopoulos^{1,3}, Evangelos Gerasopoulos¹,
5 Maria Lianou¹

6 ¹Institute for Environmental Research & Sustainable Development, National Observatory of Athens, Greece

7 ²Physikalisch-Meteorologisches Observatorium Davos, World Radiation Center, Switzerland

8 ³Department of Chemistry, University of Crete, Greece

9

10 *Correspondence to:* Dimitra Founda (founda@noa.gr)

11

12 **Abstract.** This study explores the inter-decadal variability and trends of surface horizontal visibility at the urban
13 area of Athens from 1931 to 2013, using the historical archives of the National Observatory of Athens (NOA). A
14 prominent deterioration of visibility in the city was detected, with the long-term linear trend amounting to -2.8
15 km decade⁻¹ ($p < 0.001$), over the entire studied period. This was not accompanied with any significant trend in
16 relative humidity (RH) or precipitation over the same period. A slight recovery of visibility levels seems to be
17 established in the recent decade (2004-2013). It was found that very good visibility (> 20 km) occurred at a
18 frequency of 34 % before the 1950s, while this percentage drops to just 2 % during the recent decade. The rapid
19 impairment of the visual air quality in Athens around 1950, points to the increased levels of air pollution from
20 local and/or regional emission sources, related to high urbanization rates and/or higher rates of anthropogenic
21 emissions increase on a global scale at that period. A marked seasonal cycle was detected in visibility before
22 the 1950s, which attenuates afterwards. Visibility was found to be negatively/positively correlated with relative
23 humidity (RH)/wind speed, the correlation being statistically valid at certain periods. Wind regime and mainly
24 wind direction and corresponding air masses origin was found to highly control visibility levels in Athens. The
25 comparison between visibility in Athens and at a reference, non urban site, revealed similar negative trends over
26 the common period of observations, suggesting that apart from the contribution of local sources, visibility in
27 Athens is highly determined by aerosol loads of regional origin. Satellite derived aerosol optical depth (AOD)
28 retrievals over Athens since 2000, and surface measurements of PM₁₀ confirmed the relation of visibility with
29 aerosol loads.



30

31 **1 Introduction**

32 Visibility is defined as the greatest distance at which a black object of suitable dimensions (located on the
33 ground) can be seen and recognized, when observed against the horizon sky during daylight, (WMO, 1992).
34 Visibility represents one of the dominant features of the climate and landscape of an area. Although it is highly
35 affected by atmospheric circulation and the prevailing meteorological conditions, under clear sky conditions it is
36 mainly determined from the loading of atmospheric aerosols (Davis, 1991; Lee, 1994; van Beelen and van
37 Delden, 2012; Doyle and Dorling, 2002; Singh and Dey, 2012), therefore, visibility can be a strong indicator of
38 air quality at an area. Horizontal visibility has been also introduced in formulas for the estimation of atmospheric
39 turbidity parameters (e.g. in the Ångström atmospheric turbidity coefficients, Eltbaakh et al., 2012).

40 Aerosols in the atmosphere contribute to light extinction by scattering and absorbing, thus they reduce visibility
41 (Appel et al., 1985; Chan et al., 1999; Elias et al., 2009; Singh and Dey, 2012). The impact of particulate matter
42 on visibility depends on its physical (e.g. particle size distribution) and chemical properties (Dayan and Levy,
43 2005). In particular, visibility is inversely related to light extinction coefficient, which is determined from
44 scattering and absorption of light by gases and particles, the latter (e.g. sulphate and carbon containing particles)
45 being the main contributor (Malm, 1999; Hand et al., 2002; Baumer et al., 2008; Deng et al., 2011; Wang et al.,
46 2012). Sulphate and carbon containing particles have a major role in light absorption, while the role of relative
47 humidity (RH) on visibility is also important (Larson and Cass, 1989; Malm, 1999), as when RH reaches
48 saturation values, visibility deteriorates due to fog formation and the hygroscopic growth of SO_4^{2-} , NH_4^+ and NO_3^-
49 particles (Tang, 1996; Sing and Dey, 2012). At the local to regional level, wind speed and direction are also very
50 important factors, as they determine the transport and origin of air pollution.

51 Although the use of visibility as a viable atmospheric variable has been disputed by many researchers due to the
52 numerous biases related to observational procedures (Davis, 1991), visibility statistics have been increasingly
53 used as a surrogate for aerosol loads (Zhao et al., 2011), especially since visibility records span quite long-term
54 periods. Today, there is a large number of studies that use visibility observations to investigate the spatial and
55 temporal variation of the optical properties of the atmosphere, mainly in relation to pollutants emissions and
56 aerosol loads. Studies refer to global, regional and local scales. On a global scale, a decrease of clear sky
57 visibility over land from 1973 to 2007 is reported by Wang et al. (2009). This is interpreted in terms of aerosol
58 concentrations and its impact on incident solar irradiance. A significant decrease is observed over Asia, South



59 America, Australia and Africa, while over Europe visibility increased after the 1980s, as a result of air pollution
60 mitigation measures. Vautard et al. (2009) found a significant decrease in the frequency of low visibility days in
61 Europe after the 1980s, which is spatially and temporally correlated with SO₂ emissions. Stjern et al. (2011)
62 reported that emission reductions from 1983 to 2008 in the heavily industrialized area of central Europe (the
63 formerly called Black Triangle, BT (named from the triangle of the meeting borders of Germany, Poland, and the
64 Czech Republic) caused an increase of 15 km in the horizontal visibility, in contrast to the clean area where
65 visibility increased by only 2.5 km. Doyle and Dorling (2002) observed significant improvement of visibility
66 after early 1970s at many sites in UK, attributed to changes in the use of fuels, while Van Beelen and van Delden
67 (2012) found that the proportion of days with high visibility (> 19 km) almost doubled since the early 1980s, in
68 the Netherlands. These findings for Europe are in line with the so called dimming/brightening periods, referring
69 to observed decreasing/increasing trends of surface solar radiation (SSR), associated with relevant changes in
70 anthropogenic emissions (e.g. Streets et al., 2006; Wild, 2009; Cermak et al., 2010; Folini and Wild, 2011; Nabat
71 et al., 2014).

72 In contrast to European areas, a tendency towards lower visibility is observed in developing countries (e.g. China,
73 South Korea, South Taiwan, India), where it is still difficult to control air pollution (Ghim et al., 2005; Che et al.,
74 2007; Wan et al., 2011; Singh and Dey, 2012; Wu et al., 2012). Along this line, Wu et al. (2012) found strong
75 correlation between AOD and visibility in China over the period 2000-2009, and an overall decreasing trend in
76 visibility (under sunny conditions) during the last 50 years. Singh and Dey (2012) correlated visibility in Delhi
77 with aerosol composition and reported a rapid decrease of visibility during 1980-2000, and stabilization
78 afterwards.

79 Urban environments are of particular interest, as air pollution from local sources is superimposed on other
80 regional factors, strongly impacting visibility (Davis, 1991; Eidels-Dubovoi, 2002; Tsai et al., 2003, 2007; Dayan
81 and Levy, 2005; Chang et al., 2009; Kim, 2015).

82 The present study explores the historical observations of visibility in Athens, which is the oldest time series of
83 visibility in Greece and, to our knowledge, one of the oldest, uninterrupted time series of visibility in the eastern
84 Mediterranean. The records are retrieved from the historical climatic archives of the National Observatory of
85 Athens (NOA) and span a period of more than 80 years (1931-2013). In the past, Carapiperis and Karapiperis
86 (1952) reported on the correlation between the visibility and the blue colour of the Attika sky, while
87 Kanellopoulou (1979) analysed visibility in Athens for the period 1931-1977 and reported a pronounced decrease
88 after the 1950s. Since then, there has been no other study addressing changes in visibility, as well as the factors



89 behind these changes, during the last 40 years, when significant changes occurred in Athens in terms of urban
90 expansion, traffic load, 2004 Olympic Games constructions and the economic recession (starting in 2008). The
91 inter-decadal variability and long-term trends of visibility in Athens are presented in the study. The role of
92 meteorology and aerosol loads (of local and regional sources) on the variability and trends are investigated and
93 discussed, while the relationship between visibility and aerosol loadings is investigated, through the analysis of
94 satellite AOD retrievals over Athens since 2000, but also surface measurements of PM₁₀ in Athens and Finokalia
95 station (Crete) over shorter periods.

96

97 **2 Study area and data**

98 **2.1 Study area**

99 Athens, the capital of Greece, concentrates the largest part of the commercial, financial, societal and cultural
100 activities of the country. The Greater Athens Area (GAA) (Fig. 1) extends beyond the administrative municipal
101 city limits and covers a surface of 433 km². The population of GAA is approximately 3.7 million (almost twice
102 the population of 1961) and accounts for more than one third of the Greek population. The growth of the
103 population was coupled with the number of vehicles. Specifically, the number of private cars rose from 2 % of
104 inhabitants in 1964 to 44 % in 2008. The population growth and the increased number of automobiles has caused
105 traffic problems, increased anthropogenic emissions and degradation of air quality in the city. The complex
106 topography, consisting of relatively high mountains around GAA (Fig. 1), induces poor ventilation of the city.
107 Sea/land breezes appear along the axis NE - SW and have a major role in the accumulation of air pollutants
108 (Kalabokas et al., 1999a, b).

109 In order to compare our findings for Athens with a reference, remote site, the visibility records from the
110 Heraklion airport (HER) in Crete Island, were used (Fig. 1). Heraklion is located about 330 km south of Athens,
111 while its airport is 5 km east of the city with no significant (or systematic) influence from the urban web.

112 **2.2 Climatic features of Athens**

113 Athens has a temperate climate, with warm and dry summers and more wet and mild winters, typical for eastern
114 Mediterranean. Table 1 presents monthly and annual normal values along with standard deviations of the daily
115 mean, maximum and minimum air temperature, precipitation amount and precipitation frequency (PF) (defined



116 as the number of days with total precipitation > 1 mm, following WMO), relative humidity and wind speed in
117 Athens, based on the WMO reference period, 1971-2000. July and August are the warmest and driest months of
118 the year. Actually, the periods from May to September and from October to March represent the dry and wet
119 periods of the year respectively. Precipitation is sparse in summer (June- August), with the total amount
120 averaging 20 mm and precipitation frequency averaging 3 days. Athens receives on average approximately 400
121 mm of rain per year, corresponding to 43 rainy days (Table 1).

122 During summer, the area is dominated by anticyclonic circulation that enhances air temperature and intensifies
123 urban heat island. Athens has been experiencing a significant warming since the mid 1970's, more pronounced in
124 summer, which is the additive result of regional warming and gradual intensification of the urban heat island
125 (Founda, 2011; Founda et al., 2015). Strong northeasterly winds in late summer, known from antiquity as
126 'Etesians', induce a relief on air temperature and air pollution levels in the city.

127 Figure 2b presents the seasonal variability of air masses origin over Athens according to the sectors defined in
128 Fig. 2a, based on 10-yr climatology of daily air trajectories. The S (south) sector is linked to transport of air
129 masses from arid areas of N Africa, frequently associated with dust events that affect the eastern Mediterranean
130 (Hamonou et al., 1999; Gkikkas et al., 2015), the N (north) sector accounts for Balkans and the main continental
131 Europe, while the W (west) sector corresponds to SW Europe and the W Mediterranean Basin. Note that air
132 masses transport from the W sector are significantly blocked by the high altitude mountain chain of Pindus ($>$
133 2500 m), that expands from North to South along western Greek mainland. Air masses origin was identified by
134 applying a 4-day back-trajectory analysis, calculated daily at 12:00 UT with the Hybrid Single-Particle
135 Lagrangian Integrated Trajectory (HYSPPLIT) model (version 4.9) (Draxler et al., 2009).

136 On an annual basis, air masses from the N and NE sectors dominate, contributing by more than 60 % and
137 showing profound seasonal variability (maximum in summer). Similar conclusions were obtained based on
138 surface wind speed and direction measurements reported in Fig. 3. Winds from N-NE directions prevail in Athens
139 at a frequency of nearly 38 % (Fig. 3). This sector is also associated with the occurrence of high wind speeds, as
140 shown in the same figure. The second most frequent surface winds correspond to S-SW directions (27%). The
141 frequency of occurrence of this sector maximizes during the intermediate seasons (spring and autumn) and is
142 associated with the occurrence of dust events from northern Africa and, in cases of light winds, with sea breezes
143 from the Saronic Gulf (Fig. 1).

144 2.3 Overview of air pollution in Athens



145 A short introduction on the factors that diachronically control air pollution levels in Athens is presented here, to
146 facilitate the interpretation of visibility variations in terms of pollutants concentrations.

147 Air pollution in Athens has been systematically measured since the early 1970s. Road transport, domestic
148 combustion and industrial activity have been the main sources of air pollution in GAA, throughout the years.
149 Downward trends of sulfur dioxide, black smoke, carbon monoxide and nitrogen oxides have been reported from
150 the mid 1980s to the late 1990s, attributed to several anti pollution measures adopted by the state (e.g.
151 replacement of the old technology gasoline-powered private cars and the reduction of the sulfur content in diesel
152 oil) (Kalabokas et al., 1999a). Negative trend of NO₂, NO_x and O₃ from the mid 1980s to 2009 is also reported in
153 several urban stations (Mavroidis and Ilija, 2012).

154 Measurements of particulate matter (PM) had been only occasionally conducted in Athens before the EU
155 Directive (1999/30/EC) was launched, revealing increased concentrations of PM₁₀ (Hoek et al., 1997).
156 Chaloulakou et al. (2003) reported on PM₁₀ and PM_{2.5} at a single road traffic sampling location from 1999-2000
157 and underlined the contribution of local emission sources, mostly traffic, on the high levels of PM concentration.
158 Grivas et al. (2004) highlighted the significant vehicular contributions in PM₁₀ concentrations in Athens during
159 2001-2004 and quantified the exceedances of the annual limit set by the EU Directive.

160 Studying the contribution of local sources versus regional and the role of long-range transport over megacities of
161 the eastern Mediterranean, including GAA, Kanakidou et al. (2011) summarized that a significant number of PM
162 exceedances registered in Athens, are associated with regional pollution sources or natural dust transport, clearly
163 highlighting the importance of regional transport processes. Theodosi et al. (2011), compared simultaneous mass
164 and chemical composition measurements of size segregated particulate matter (PM₁, PM_{2.5} and PM₁₀) at two
165 urban and a reference, non-urban background site, concluding that, during the warm season there is no significant
166 (actually < 15 %) difference in PM₁ between the urban and reference sites, while on the other hand, local
167 anthropogenic sources dominate during the cold season. Regarding the coarse fraction, a significant contribution
168 from soil was found in urban locations throughout the year, contributing significantly (up to 33 %) to the local
169 PM₁₀ mass.

170 Regarding columnar aerosol loads and using ground-based AOD measurements in Athens, Gerasopoulos et al.
171 (2011) showed that the greatest contribution (40 %) to the annually averaged AOD, comes from regional sources
172 (namely the Istanbul metropolitan area, the extended areas of biomass burning around the north coast of the
173 Black Sea, power plants spread throughout the Balkans and the industrial area in the Po valley). Additional



174 important contributors are dust from Africa (23 %), whereas the rest of Europe contributes another 22 %. Gkikas
175 et al. (2015) found good correlation between AOD_{550nm} and surface PM_{10} over the Mediterranean basin during
176 desert dust episodes (2000-2013) and reported higher intensity but lower frequency of such episodes over the
177 central and eastern Mediterranean. Additionally, Hatzianastassiou et al. (2009) found that local anthropogenic
178 emissions in GAA contribute by 15-30% to the total AOD, as derived from satellite-based AOD measurements.

179 Vrekoussis et al. (2013) reported on the improvement of air quality in Athens during the period 2008-2013, as a
180 result of the economic recession and the subsequent cut down on vehicles use and industrial activity. For the
181 same period, Paraskevopoulou et al. (2014) showed that the massive turn of Athens' population to wood burning
182 for residential heating purposes gave rise to smog episodes characterized by high PM spikes during night time in
183 winter. A longer-term (2008-2013) analysis of aerosol chemical composition and sources at a suburban site in
184 Athens by Paraskevopoulou et al. (2015) revealed that the area of Athens is now generally dominated by aged,
185 transported aerosols.

186 **2.4 Visibility observations in Athens**

187 The historical climatic records of the National Observatory of Athens (NOA) were used in this study. NOA is
188 established on the Hill of Nymphs (latitude: 37.97 °N, longitude: 23.71 °E, altitude: 107 m, above sea level), at
189 the historical center of the city, near Acropolis. The location of the observations on the top of a hill ensures
190 unobstructed view towards all directions. Visibility observations have been conducted uninterruptedly at NOA at
191 least 3 times per day, since the late 1920's. Daily observations of visibility at 14:00 LST (LST = UT + 2hrs),
192 from 1931 to 2013 were used in the study. The time series is complete, with a very short gap of 6 days occurring
193 in December 1944, owed to political convulsion in the country at that period.

194 Visibility data at other stations (e.g. Heraklion, Crete) were extracted from the network of the Hellenic National
195 Meteorological Service (HNMS) and actually represent visibility observations at the airport station, initiated after
196 mid the 1950s. Meteorological data for Athens over the period 1931-2013, were also acquired from the historical
197 archives of NOA. Monthly, seasonal and annual mean values of visibility were derived from the daily
198 observations at 14:00 LST.

199 An empirical scale of visibility classes, as recommended by the World Meteorological Organization (WMO), has
200 been used for visibility observations at NOA (Table 2). Classes are defined based on the greatest distance at
201 which a predefined object can be seen and recognized with naked eye. The procedure requires that an operator



202 scans the horizon for predetermined objects. In the case of Athens, some historical buildings in the city, but also
203 certain objects of the surrounding landscape, unaltered over the years, (e.g. objects on the mountains or islands of
204 the Saronic Gulf, Fig. 1), were chosen to represent visibility classes and relevant distance ranges. The procedure
205 inevitably introduces some kind of subjectivity and bias in the measurements, related to individual eyesight of
206 different operators. It is assumed however, that the execution of visibility observations by different operators over
207 the years could have possibly had a compensating effect and an overall reduction of biases. More details about
208 the possible errors and validity of visibility observations have been thoroughly discussed by Davis, (1991).

209 The use of the WMO scale introduces a further uncertainty on visibility observations, associated with the
210 amplitude of visibility ranges corresponding to each visibility class. Information on the use of WMO scale and
211 relative uncertainties, as well as the procedure followed for averaging daily visibility observations is provided in
212 Supplementary materials.

213 **2.5 Aerosol data used in the study**

214 Long time series of atmospheric pollution measurements in Athens and the selected reference site would enable
215 drawing direct relationships between visibility and aerosols and would provide evidence on the character
216 (regional or local) of atmospheric pollution in Athens and its impact on long-term visibility variations. Given that
217 such time series are missing, we used shorter time series of aerosol measurements for a direct comparison
218 between visibility and atmospheric pollution in Athens.

219 In an effort to explore the relationship of visibility with AOD over Athens, we used the Terra/Modis AOD at 550
220 nm, available since 2000. NASA's Terra satellite is sun synchronous and near polar-orbiting, with a circular orbit
221 of 705 km above sea level. MODIS is capable of scanning 36 spectral bands across a swath 2330 km wide.
222 MODIS aerosol products were used in order to analyze the temporal and spatial variability of aerosols over the
223 wide area of interest. In this study, we used daily level-2 collection 5.1 MODIS/Terra AOD at 550 nm. Daily
224 overpass data for the specific area were extracted at a spatial resolution of 50 x 50 km². Previous studies have
225 shown that such special resolution product ensures sufficient daily measurements without losing out to the higher
226 spatial resolution and hence provide a better opportunity of correctly viewing the atmospheric aerosol load
227 (Ichoku et al., 2002). The overpass time is 09:35 ± 45 min UT.

228 Surface PM₁₀ measurements in Athens were also used to verify the relationship between visibility and
229 particulate pollution from surface measurements. It is well known that desert dust plumes are often transported in



230 altitude over the Mediterranean (e.g. Hamonou et al., 1999; Gkikkas et al., 2015) and a portion of surface PM
231 exceedances in Athens is associated with natural dust transport (Kanakidou et al. (2011)). The analysis was based
232 on a short data set of PM₁₀ measurements at two stations in Athens (Aristotelous and Maroussi), covering the
233 period 2008-2012. Aristotelous is an urban street station in the center of the city and Maroussi is a suburban
234 station, at a distance of about 15 km to the North of NOA.

235 Finally, a data set of PM₁₀ measurements at a reference station in Crete (Finokalia station), covering the period
236 2005-2014 was used, for the detection of any trends, representative of regional atmospheric pollution trends.
237 Finokalia station is located at a distance of less than 50 km East of Heraklion airport.

238

239 **3 Results**

240 **3.1 Inter-decadal variation of visibility and trends**

241 Figure 4 displays the long-term evolution and variability of the annual visibility in Athens from 1931 to 2013.
242 The population growth in the city of Athens over the same period is also shown, while the figure also displays the
243 long-term variability of the relative humidity in Athens (which is discussed below). It is obvious that the annual
244 visibility in Athens has undergone a very strong and almost continuous decline over the past 80 years, in
245 coincidence with the increase in population. The long-term linear trend over the whole studied period was found
246 to be equal to $-2.8 \text{ km decade}^{-1}$ ($p < 0.001$). However, this trend is not constant throughout the entire studied
247 period. Three sub-periods are visually discerned in Fig. 4 (also confirmed with sensitivity tests): (a) 1931-1948,
248 (b) 1949-2003 and (c) 2004-2013. Visibility levels are remarkably higher in the first sub-period varying around
249 25 km. A slight negative trend is observed during this period ($-0.66 \text{ km decade}^{-1}$). In the late 1940s, visibility
250 experienced a striking and abrupt decrease at the time of population first burst, which was then followed by a
251 progressive deterioration, at least until the early 2000s. In this second sub-period (1949-2003) visibility decreases
252 at a rate of $-2.33 \text{ km decade}^{-1}$ ($p < 0.001$). A tendency of stabilization or even recovery seems to be established
253 during the recent decade 2004-2013, with visibility showing a slight increasing trend ($+0.07 \text{ km yr}^{-1}$). A detailed
254 discussion on the observed trends and their linkage with air pollution is presented in section 3.5.

255

256 **3.2 Frequency distribution of visibility ranges**



257 Figure 5 illustrates the frequency of occurrence of different visibility ranges as described in Table 2 for the three
258 sub-periods. In the first sub-period, visibility values lie within the range of 10-20 km at a percentage of 36 % and
259 of 20-50 km at a percentage of 34 %. Very high visibility (>50km) accounts for a considerable percentage (~9 %) and
260 poor visibility (< 2 km) corresponds cumulatively to only 2 %. The frequency of visibilities lower to 1 km is
261 very low (0.4 %), while visibility was found to be lower to 500 m only in 9 cases. Cumulatively, visibility
262 exceeding 10 km corresponds to approximately 80 % of the cases during this period.

263 A shift towards lower visibility values is observed during the second sub-period, namely 1949-2003. Specifically,
264 the most frequent visibility ranges are 4-10 km (38 %) and 10-20 km (34 %). The frequency of visibility > 50 km
265 is negligible (0.6 %) and the frequency of poor visibility (< 2 km) amounts cumulatively to 5.6 % , with 0.9 %
266 corresponding to visibility < 1 km. Visibility lower to 500 m was observed only in 12 cases. Cumulatively, the
267 percentage of days with visibility exceeding 10km drops to 45 % during this sub-period.

268 The frequency distribution changes dramatically during the most recent period (2004-2013). In particular,
269 although visibility range of 4-10 km remains the most frequent (30%) as in the second sub-period, almost similar
270 frequency (~28 %) is also observed in the range of 2-4 km, corresponding to a doubling of the percentage of this
271 category. The frequency of poor visibility (<2km) rises to approximately 25 %, with a substantial percentage (5.6
272 %) accounting for visibility lower to 1 km and 0.46 % lower to 500 m. Cumulatively, visibility did not exceed 4
273 km for half of the days of the year during 2004-2013. The percentage of days with visibility > 10 km is 18%,
274 while frequency of very good visibility (> 20 km) amounts to just 2 %. No case of visibility > 50 km was
275 observed in this sub-period.

276 3.3 Seasonal variation of visibility

277 Since visibility is influenced by the prevailing meteorological conditions (Davis 1991; Sloane 1982), it is
278 expected that it will also exhibit a seasonal variability, depending on the intra annual variability of climatic
279 conditions at the examined area. Mean monthly values of visibility were calculated for all three sub-periods.
280 Figure 6 presents the mean monthly values of visibility in Athens over the three sub-periods, normalized with the
281 value of the month with the highest visibility. In the same plot, the mean monthly values of the relative humidity
282 (RH), coinciding visibility observations at 14:00 LST over the period 1931-2013, are also shown. It is noteworthy
283 that RH at NOA does not exhibit any significant trend over the years (as already shown in Fig. 4) and its monthly
284 distribution is almost unaltered over the years. As it comes out from Fig. 6, visibility shows a distinct seasonal
285 cycle in all three sub-periods, with better visibility occurring in the warm and dry season of the year. Although



286 seasonality is observed in all sub-periods, the pattern is more evident and robust in the first sub-period, with
287 much higher visibility values (up to 40%) in the warm and dry months compared to cold and wet months. The
288 pattern of visibility in this period is almost a mirror image of the pattern of RH and reflects the influence of RH
289 on visibility and the anti-correlation between these two variables. The lowest values of RH correspond to July
290 and August (mean value of RH ~35%) and this probably results to improvement of visibility. Moreover, strong
291 northeastern winds (the so called ‘Etesians’) that prevail in eastern Greece during these months enhance
292 ventilation and induce drier conditions in the city, therefore improving visibility.

293 In the other two sub-periods, 1949-2003 and 2004-2013, higher visibility values are also observed during the
294 warm and drier months (Fig. 6), however, the distinct seasonal cycle observed in the first sub-period has changed.
295 During the second sub-period in particular, seasonality is noticeably attenuated and visibility differences between
296 the warm and cold period is of the order of 10%. This possibly implies a weakening of the influence of
297 meteorological conditions as a result of (or in combination with) stronger effect of air pollution on the visual air
298 quality of the city.

299 The minimum of visibility is constantly observed in March during all sub-periods. Indeed, March falls in the
300 transitional season of the year and thus bears higher values of RH compared to summer months (mean value of
301 RH at 14.00 LST > 50 % and mean daily value 67 % in March). Additionally, March falls in the growing season,
302 with enhanced pollen and biogenic aerosol emissions which is a known factor for visibility impairment (e.g. Kim,
303 2007). Increased frequency of dust outbreaks from northern Africa in spring, influence extensively the area of
304 eastern Mediterranean (Hamonou et al., 1999; Gerasopoulos et al., 2005, 2011; Gkikkas et al., 2015) and thus
305 constitute a major factor for visibility impairment during spring months. Léon et al (1999) reported that ~ 40 % of
306 the days with high aerosol optical depth at 865 nm ($AOD_{865nm} > 0.18$) over Thessaloniki (Greece) were
307 associated with African dust transport events, all observed in the period March - July, while Dayan and Levy
308 (2005) found higher PM_{10} values and lower visibility levels during spring in Tel Aviv, associated with the
309 frequent passage of cyclones that cause natural dust outbreaks.

310 **3.4 Visibility and meteorological conditions**

311 The impact of meteorological conditions on visibility has been investigated by different researchers using
312 different approaches, as for instance the classification of synoptic circulation patterns (Sloane, 1982; Davis,
313 1991; Dayan and Levy, 2005), the application of correction factors on extinction coefficient to account for RH
314 effect (Che et al., 2007), the estimation of correlation coefficients between visibility and meteorological variables



315 (Deng et al., 2011), or simply the comparison of diurnal /seasonal cycles and temporal trends of visibility with
316 the relevant cycles and trends of meteorological variables (Van Beelen and van Delden, 2012). Sloane (1982)
317 reported that periods with exceptionally maxima or minima of visual air quality were related (apart from sulphate
318 emissions) with favourable synoptic circulation patterns. Studying visibility in Tel Aviv (Israel), Dayan and Levy
319 (2005) reported a strong dependence of visibility levels from meteorological conditions, synoptic weather
320 patterns and air mass origin, with the highest mean values occurring in summer, related to the persistent nature of
321 the summer synoptic weather pattern in the eastern Mediterranean. Deng et al. (2011) found that RH and wind
322 speed were significantly correlated with visibility at an urban area of China, while Ghim et al. (2006) showed a
323 considerable decrease in visibility in South Korea, despite the observed simultaneous decrease of the relative
324 humidity levels. The relationship and possible impact of different meteorological parameters such as
325 precipitation, RH, wind speed and wind direction on visibility in Athens is discussed below.

326 **3.4.1 Visibility and precipitation**

327 Precipitation is associated with scavenging of atmospheric particles (e.g. Remoudaki et al., 1991a; 1991b),
328 possibly resulting to improvement of visibility. The precipitation frequency in particular, was found to control
329 seasonal variability of the total atmospheric deposition of lead in western Mediterranean (Remoudaki et al.,
330 1991b). Rainy days on the other hand are associated with increased relative humidity, resulting in reduction of
331 visibility. A plot illustrating the long-term variability of the annual precipitation amount and precipitation
332 frequency (PF) at NOA from 1931-2013 was created, for the detection of any significant temporal trends which
333 might have an effect on visibility trends (Fig. 7). According to Fig. 7, no long-term trend is observed in the
334 annual precipitation amount at NOA from 1931-2013, which could have had an effect on long-term trends of
335 visibility. Precipitation frequency on the other hand exhibits an overall negative trend over the same period (-1.1
336 days decade⁻¹), not constant, though. Actually, PF decreases from the late 1960s to the late 1980s, while it
337 presents an increasing tendency after 1990 (+1.3 days decade⁻¹). The correlation coefficient between annual
338 visibility and PF was found to be positive only during the period from early 1970s to the late 1980s (+ 0.45, $p <$
339 0.05). A negative correlation coefficients was found in the post 1990 period (-0.21), not statistically significant.

340 Subsets of data were also produced for the creation of additional visibility time series, accounting for
341 precipitation influence. Figure 8 presents visibility variability during the wet (October-March) and dry (May-
342 September) period of the year, along with the annual values. Lower values during the rainy and cold period of the
343 year are most probably associated with higher values of relative humidity, resulting to reduction of visibility.



344 Despite the differences between the time series in Fig. 8, the overall tendency is similar, thus not affecting the
345 validity of our conclusions as regards long-term visibility impairment in Athens. Additional plots created from
346 subsets of ‘rain’ and ‘no rain’ days are provided in Supplementary materials (Fig. S4).

347 **3.4.2 Correlation between visibility and other meteorological parameters (RH, wind)**

348 Figure 9 presents the running correlation coefficient (15-yrs window) between visibility and relative humidity,
349 over the period 1931-2013. As expected, the correlation coefficient between visibility and RH is negative,
350 indicating the anti-correlation between these two variables. High RH enhances water uptake by airborne particles,
351 leading to higher light scattering and thus visibility impairment. Actually, when RH exceeds a threshold level
352 (e.g. > 70%) some inorganic salts, such as ammonium sulfate and nitrate, undergo sudden phase transitions from
353 solid particles to solution droplets and become disproportionately responsible for visibility impairment, as
354 compared with other particles that do not uptake water molecules (Malm, 1999).

355 As it comes out from Fig. 9, the negative correlation between RH and visibility is statistically significant ($p <$
356 0.01) almost over the entire studied period. However, a progressive weakening of the correlation coefficient with
357 time is observed, indicating a less strong correlation between the two variables over the years. Stronger anti-
358 correlation is found until early 1970s, followed by lower (still significant) values till late 1970s. The progressive
359 weakening of the correlation between RH and visibility in Athens, possibly suggests a progressive weakening or
360 mask of the influence of RH on visibility, compared to the effect of other factors such as atmospheric pollution
361 (although the influence of RH is enhanced in the presence of certain hygroscopic particles). On the contrary, the
362 impact of surface wind speed on visibility seems to be stronger during the recent decades (Fig. 9). Higher wind
363 speeds in this case (positive correlation) are related to the dispersion of air pollutants and the more efficient city
364 ventilation. In others cases wind speed is also used as a proxy for long-range transport, but then a negative
365 correlation would be expected. Lower values of the coefficient in the first decades possibly demonstrate that the
366 lack of pollutants at that period diminishes the importance of ventilation. The correlation coefficient
367 progressively increases over the years. The rate of increase is higher after the mid 1980s, when correlation
368 becomes statistically significant ($p < 0.01$). Similar values (~ 0.29) of correlation coefficient between light
369 extinction coefficient and wind speed are reported by Deng et al. (2011) in China.

370 Apart from wind speed, visibility was also found to be sensitive to wind direction. A distinct variability of
371 visibility with wind direction is observed in Fig. 10, for all sub-periods. Lower values of visibility are related to
372 southerly winds, as they either bring dust from Sahara or warmer and more humid air masses from the sea (see



373 also Figs 1, 2b). Southeasterly winds are in general weak winds (see Fig. 3), while southwesterly winds are
374 associated with sea breezes from the Saronic Gulf (Fig. 1). In general, sea breeze and calms favor the
375 accumulation of pollutants, the formation of secondary aerosols and photochemical smog in Athens (Colbeck et
376 al., 2002), thus reducing visibility. A number of S/SW events are also associated with strong wind speeds
377 occurring during Sahara dust outbreaks, which enrich Athens atmosphere with dust particles that decrease
378 visibility (Figs 2, 3). As it comes out from Fig. 10, the highest visibility occurs under northwesterly winds and
379 this is robust over the entire studied period. An explanation for this, is that air masses originated from
380 northwesterly directions are much drier as they have lost water vapor after passing over the high mountainous
381 basin of Greek mainland (e.g. Pindos mountain), while air pollution is also blocked within the boundary layer by
382 the mountain chain.

383 **3.5 Air pollution and urbanization relations to visibility**

384 In this section we attempt to interpret the observed inter-decadal variability and trends of visibility in Athens, in
385 terms of air pollution. As already shown in Fig. 4, the pre-1950 period is characterized by much better visibility
386 in Athens. From then on, visibility experienced a rapid decrease, followed by a smoother but continuous negative
387 trend until the early 2000s. The period after 1950 signifies the post World War II epoch but also coincides with
388 the end of a civil war in Greece (1946-1949), which was followed by an important urbanization wave in Athens
389 (Maloutas, 2003). This is in line with the growth of Athens' population, as illustrated in Fig. 4. The greatest rate
390 of population increase is observed between 1950 and 1960, when population in Athens almost doubled. The
391 population growth was associated with a significant increase of constructions in the city. Apart from the intense
392 urbanization in Athens, this period is also characterized by the most prominent increase of anthropogenic
393 emissions on a global and European scale (e.g. Mylona, 1996; van Aardenne et al., 2001), which is discussed
394 below.

395 Although in the second sub-period, 1949-2003, visibility was found to be remarkably lower compared to the first
396 one, a slight recovery of visibility was observed during the recent decade, 2004-2013 (Fig. 4). This improvement
397 could be related to a number of reasons. The years after 2004 correspond to the post Olympic Games period in
398 Athens. A number of important transport projects were completed prior to the Olympic Games in Athens in 2004.
399 Such projects are for instance the construction of the Attika Ring Road (one of the largest in Europe), the
400 construction of Tramway and the extension of Athens Metro. These projects have contributed to the reduction of
401 the number of vehicles in the city, resulting to less traffic problems and lower air pollution levels. Another



402 possible contributing factor concerns the possible impact of the Greek economic recession (2008-2013) on air
403 quality in Greece, and Athens in particular. Recent studies provide some evidence for this. For instance,
404 Vrekoussis et al. (2013) found strong correlation between different economic metrics and air pollutants after
405 2007, suggesting that the economic recession has resulted in proportionally reduced levels of air pollutants in the
406 two biggest cities in Greece. This is further supported by other recent research studies that report a significant
407 reduction in energy consumption after 2008, related to the rapid economic degradation (Santamouris et al., 2013).

408 But how far are these changes in visibility in Athens due to local factors or can be considered representative of a
409 more extensive area? To answer this question and also evaluate our findings as regards the urban influence, the
410 Athens visibility record is compared with visibility at a reference, non urban station. From the available stations
411 in Greece disposing long-term visibility observations, we chose the station at Heraklion airport (HER) in Crete
412 Island. Actually, both sites, NOA and HER, are most of the year exposed to air masses of similar origin (from
413 northeasterly directions), travelling over the Aegean Sea, in contrast to other sites of the country that are strongly
414 affected by the mountainous volumes of the Greek mainland. Visibility observations at HER are available since
415 the mid 1950s. Figure 11 presents the long-term variation of the annual visibility at HER along with annual
416 visibility at NOA. Linear trends of the two time series for their common period (1956-2009) are also shown in the
417 figure. The time series were found significantly correlated (correlation coefficient >0.88 , $p < 0.05$).

418 As it comes out from Fig. 11, visibility levels at urban NOA are constantly lower by a few km (~ 7 km) compared
419 to the background station, HER. It is remarkable that during the first two decades of parallel observations, both
420 curves show significant covariance, easily realized from the peaks in 1959, 1966 and 1970 and the minima in
421 1963 and 1973, suggesting the impact of large scale phenomena (for instance, volcanic eruptions in 1963) in the
422 modulation of visibility levels. A prominent feature in Fig. 11 is that the background visibility at the reference
423 site has been also on a downward route since the mid 1950s, in accordance to the observed decreasing trend of
424 the visibility in Athens. As already stated, the beginning of the 1950s signifies a period with an outstanding
425 increase of emissions in Europe. European SO_2 emissions in particular, increased almost at a constant rate during
426 the first half of the 20th century, while they experienced a quite abrupt increase in the 1950s and almost doubled
427 their values between 1950 and 1960 (van Aardenne et al., 2001; Mylona, 1996). Figure 11 includes the rates of
428 SO_2 increase per decade in Europe (in Tg S decade^{-1}), as reported by van Aardenne et al. (2001). Constant
429 increasing rates ($2 \text{ Tg S decade}^{-1}$) are observed until 1950, when the rate of increase reached $6 \text{ Tg S decade}^{-1}$
430 between 1950-1970. A decline of the increasing rate is then observed, while in the 1990s European sulfur
431 emissions stabilize. Stabilization of emissions is followed by a continuous decline after 1990. Stjern et al. (2011)



432 reported a prominent decrease of SO_x emissions and sulphate in aerosols in both eastern and western Europe from
433 1990-2007, but with higher rates of decrease in eastern Europe.

434 A very important finding in Fig. 11 is the similar slopes in the linear trends of the annual visibility at the
435 background and urban stations, over their common period of observations (-2.2 km decade⁻¹ and -2.4 km decade⁻¹,
436 respectively). This feature implies that, apart from the absolutely lower values of visibility in the urban web of
437 Athens, the inter-decadal variability of visibility in the city and the extended area is significantly modulated by
438 large scale processes that control regional visibility, such as long-range pollution transport and/or changes of
439 atmospheric circulation. Many studies have identified the eastern Mediterranean as a crossroad of aerosols of
440 different origins, sizes and chemical composition (Lelieveld et al., 2002; Hatzianastassiou et al., 2009; Kanakidou
441 et al., 2011; Gerasopoulos et al., 2011), which inevitably affect optical properties of the atmosphere. Kanakidou
442 et al. (2011) found that even in the large urban regions of the eastern Mediterranean, particulate matter has a
443 significant contribution by distant anthropogenic pollution sources in the region but also by long-range transport
444 of African dust.

445 After the early 1990s, the time series diverge, with background visibility partly recovering, and visibility in
446 Athens keeping declining at the same pace until 2003 (Fig. 11). Recovering of visibility at other Greek areas
447 around the 1990s is also found by Lianou et al. (unpublished data) which is also in line with the observed
448 visibility improvement in other European areas, related to emissions reduction (Wang et al., 2009; Vautard et al.,
449 2009). This last feature suggests that during this period, local emissions might have a dominant role in the
450 determination of visibility in Athens.

451 **3.6 Visibility in Athens and AOD**

452 The relationship of visibility with AOD over Athens was also explored using satellite data since 2000 (see
453 Section 2.5). The AOD time series showed a significant (-2.4% per year) decrease from 2000 up to 2010 and a
454 further decrease of (-7.4% per year) for the 2010-2014 period (Fig.12).

455 To investigate the relationship between visibility and AOD changes, the two parameters are plotted together after
456 data binning. Visibility and AOD measurements have been used as follows: Visibility at 12:00 UT was used
457 according to the indices defined in Table 2 and plotted against average AOD from synchronous satellite
458 overpasses. The mean AOD and its standard deviation are presented in Fig. 13. The AOD values are related with
459 the visibility data using as the distance in km the middle point of each visibility bin (range). Only summertime



460 (June-August) MODIS AOD have been used, to keep visibility values unaffected from other atmospheric
461 parameters like low clouds, rain or relative humidity. It is observed that for average AOD values for Athens (0.25
462 using the mean June-August AOD at 550nm from our MODIS AOD dataset or 0.23 at 500 nm as reported by
463 Gerasopoulos et al., 2011) visibility varies in the range of 4 km to 10 km. For cleaner conditions (W-NW-N, 0.12
464 - 0.17 at 500 nm, Gerasopoulos et al., 2011) visibility can go as high as 20 km, while very low visibility (< 0.5
465 km) is generally associated to the highest aerosol loads, with AOD > 0.3 (e.g. in the case of dust events, long-
466 range transport of urban/industrial pollutants and stagnant conditions).

467 **3.7 Visibility in relation to PM₁₀**

468 An additional analysis was conducted to verify the relationship between visibility and particulate pollution from
469 surface measurements using a short data set of PM₁₀ in Athens as described in Section 2.5. Figure 14 presents
470 visibility variation as a function of PM₁₀ levels measured at Aristotelous (urban) and Maroussi (suburban)
471 stations. Four different classes of PM₁₀ levels were used, as shown in Fig. 14. The frequency of occurrence of
472 each class is also shown in the figure. Despite the different locations and characteristics of the two stations, the
473 observed frequencies are very similar in all classes of PM₁₀ levels, with higher frequency corresponding to the
474 class of 30 -60 $\mu\text{g m}^{-3}$ at both stations. The frequency of PM₁₀ > 90 $\mu\text{g m}^{-3}$ at Aristotelous is double compared to
475 the respective frequency at Maroussi. Independently of the location, the same strong relationship is observed
476 between visibility reported at NOA and PM₁₀ levels at both stations, revealing a prominent decrease of visibility
477 with increasing PM₁₀ levels, in agreement with our conclusions. Average visibility at NOA ranged between 8 and
478 9 km under low PM₁₀ levels (< 30 $\mu\text{g m}^{-3}$), but is reduced to less than 3 km under severe episodes of particulate
479 pollution (PM₁₀ > 90 $\mu\text{g m}^{-3}$). The correlation coefficient between daily measurements of PM₁₀ levels and daily
480 visibility at NOA was found equal to -0.38 ($p < 0.05$) and -0.36 ($p < 0.05$) for Aristotelous and Maroussi sites
481 respectively.

482 Figure 15 displays the variation of the mean annual values of PM₁₀ at the reference station of Finokalia (Crete)
483 over the 10-yr period (2005-2014), along with standard deviations. A decreasing tendency in PM₁₀ levels is
484 observed, which is also consistent with the slight recovery of visibility levels in Athens over the same period.

485

486 **4 Discussion and Conclusions**



487 The present work analyses for first time the historical record of visibility in Athens (NOA) from 1931 to 2013
488 and explores its long-term variability and trends. An attempt was made to interpret the temporal variations of
489 visibility in terms of relevant changes of atmospheric properties (related to local or regional processes) and/or
490 meteorological conditions. Since this is the longest record of visibility observations in Greece and one of the
491 oldest in the broader area of the eastern Mediterranean, the analysis provided valuable information on the
492 atmospheric properties of the area in the past, when air pollution records were missing.

493 The study period was divided into sub-periods corresponding to different visibility trends in the time series, each
494 sub-period being affected by different factors.

495 The role of meteorology on visibility was investigated in different ways. Visibility in Athens was found to reveal
496 a distinct seasonal cycle, with higher visibility corresponding to the warm and dry months of the year (namely
497 from May to September) and lower to the colder and wet months. Seasonality is more evident in the first sub-
498 period, when visibility in summer is up to 40% larger compared to winter. After the 1950s, the seasonal cycle
499 attenuates and the differences in visibility between summer and winter months were found to be much less
500 pronounced (of the order of 10%, Fig. 6). Lower visibility values were observed in March in all sub-periods,
501 resulting from the combination of enhanced pollen and biogenic aerosols emissions, but also to increased dust
502 outbreaks from northern Africa and relatively higher RH levels.

503 As expected, visibility was found to be negatively correlated with RH, but correlation is stronger in the first sub-
504 period and attenuates over the years. On the contrary, a positive correlation between visibility and wind speed
505 was detected which is statistically significant ($p < 0.01$) only during recent decades. Actually, stronger winds
506 seem to improve visibility as they induce a cleanup of the atmosphere from air pollutants.

507 Visibility was found to be very sensitive to wind direction, reflecting the influence of air masses origin. Lower
508 visibility levels are constantly observed under southerly winds (Fig. 10). Such winds correspond to sea breeze
509 circulation associated with increased humidity levels but also to accumulation of air pollutants in the city and
510 formation of secondary air pollutants. In addition, some S/SW events are associated with strong wind speeds
511 (Fig. 3) occurring during Sahara dust outbreaks. These events enrich Athens with airborne particles, thus
512 decreasing visibility.

513 The study demonstrated that visibility in Athens has undergone a prominent impairment since the early 1930s.
514 The overall trend of annual visibility averages amounts to $-2.8 \text{ km decade}^{-1}$. The impressively higher levels of
515 visibility in Athens before the 1950s (also characterized by strong seasonality) reflect the transparency of the



516 atmosphere at that period, inherent to poorer aerosol loads from anthropogenic emissions (urban and/or regional).
517 The dramatic decrease of the visual air quality in the 1950s coincides with a number of events (end of wars, rapid
518 urbanization, increased emissions on local and regional scale) and points to the prominent role of aerosol loads in
519 the atmosphere of Athens. Air pollution has gradually incurred a severe visual pollution in the city, with visibility
520 lower to 4 km observed during more than half of the year in the recent decade, 2004-2013. The significant
521 decrease of visibility in Athens was not accompanied with analogous significant trends in RH or precipitation
522 (Figs 4, 7).

523 The comparison of the annual visibility in Athens with visibility at a reference, non urban site (HER) in Crete,
524 revealed some very interesting features. First, visibility in Athens was found to be constantly lower compared to
525 HER, possibly suggesting the impact of local anthropogenic emissions in the urban web. However, both time
526 series revealed similar and significant negative trends over their common period of observations (after the mid
527 1950s), pointing to the major contribution of long and regional range transport of natural and anthropogenic
528 pollution sources in the GAA urban area. Visibility deterioration after the mid 1950s is also reported in most
529 European areas, followed by stabilization and/or improvement around the 1980s or later (Vautard et al., 2009;
530 van Beelen and van Delden, 2012; Stjern et al., 2011). An improvement of visibility at HER around the 1990s
531 was not associated with analogous improvement of visibility in Athens, where visibility deterioration continued
532 until the early 2000s (Fig. 11). At that period, negative trends of main gaseous air pollutants are reported in
533 Athens (Kalabokas et al., 1999a). However, the direct effect of such pollutants on light extinction is negligible
534 compared to suspended particles and particularly to fine particles ($< 1\mu\text{m}$).

535 As already stated in Section 2.3, the contribution of both local and distant emission sources in PM concentrations
536 in Athens is suggested by a number of studies (e.g. Kanakidou et al., 2011; Gerasopoulos et al., 2011). Mainly
537 local emission sources (e.g. traffic) have been found to contribute to PM_{10} concentration (Chaloulakou et al.,
538 2003; Grivas et al., 2004), while local anthropogenic sources seem to control PM_1 concentration only during the
539 cold months of the year (Theodosi et al., 2011). Using satellite-based AOD measurements, Hatzianastassiou et al.
540 (2009) found that local anthropogenic emissions in GAA contribute up to 30% to the total AOD.

541 A strong anticorrelation was found between visibility at NOA and PM_{10} levels, measured at two different stations
542 (urban and suburban) in Athens over the period 2008-2012 (Fig. 14). The relationship between AOD and
543 visibility in Athens was examined in the study (Figs 12, 13). Illustrating the relationship between AOD, which
544 consist in a vertically integrated parameter, and visibility, a horizontally integrated parameter, requires various
545 assumptions. Using satellite based AOD and visibility observations for GAA, when assuming a vertically



546 constant extinction coefficient and a mixing layer that contains all aerosol load we end up describing the
547 theoretical relationship (Koschmieder, 1924): $Vis = k / AOD$, where k is a function of the mixing layer height.

548 The 82-years long time series of visibility in Athens unfolded for first time information on the atmospheric
549 conditions in the area, for periods when atmospheric pollution measurements are missing. Although the analysis
550 is subject to several limitations and assumptions, mainly related to methods of visibility observations, the results
551 are robust and statistically significant, as the outstanding degradation of the visual air quality in the city over the
552 years.

553 The observed stabilization (or even slight improvement) of visibility in Athens in the very recent years could
554 possibly be related to reduced local anthropogenic emissions as a result of important transport infrastructures
555 (executed in view of Olympic Games) but also of the economic crisis in Greece. Although this last argument is
556 already supported by some recent research studies (e.g. Vrekoussis et al., 2013; Santamouris et al., 2013), the
557 impact of the economic crisis on local emissions seems to be more complicated and drawing out conclusions
558 remains tentative. Besides, in the same period regional atmospheric pollution presents a decreasing tendency, as
559 reflected in the negative trend of PM_{10} levels measured at the background station of Finokalia in Crete (Fig. 15)
560 which is also consistent with the recent recovery of visibility in Athens.

561

562 **Acknowledgments.** The study is a contribution to the ChArMEX (The Chemistry-Aerosol Mediterranean
563 Experiment) work package on variability and trends. The study was supported by the Excellence Research
564 Program GSRT- Siemens (2015-2017) ARISTOTELIS "Environment, Space and Geodynamics/Seismology
565 2015-2017" in the framework of the Hellenic Republic-Siemens settlement Agreement. The authors are grateful
566 to the Editor Dr. François Dulac, for his very useful comments and suggestions on this study. The authors would
567 like also to thank the Hellenic National Meteorological Service (HNMS) for the provision of visibility data at
568 Heraklion (Crete) and the Air Quality Department of the Ministry of Environment & Energy of Greece for the
569 provision of air pollution data. The contribution of Mr. F. Pierros (NOA) and Mrs D. Koutentaki (NOA) in the
570 digitisation of visibility data of NOA and of Dr. G. Kouvarakis (University of Crete) in the analysis of air
571 trajectories is also acknowledged.

572

573 **References**



- 574 Appel, B.R., Tokiwa, Y., Hsu, J., Kothny, E., and Hahn, E.: Visibility as related to atmospheric aerosol
575 constituents, *Atmos. Environ.*, 19, 1525-1534, doi:10.1016/0004-6981(85)90290-2, 1985.
- 576 Bäumer, D., Vogel, B., Versick, S., Rinke, R., Möhler, O., and Schnaiter, M.: Relationship of visibility, aerosol
577 optical thickness and aerosol size distribution in an ageing air mass over South-West Germany, *Atmos. Environ.*,
578 42, 989-998, doi:10.1016/j.atmosenv.2007.10.017, 2008.
- 579 Carapiperis, L.N., and Karapiperis, P.P.: On the ocean colour of the sky in Athens, *Academy of Athens*, 27, 213,
580 1952.
- 581 Cermak, J., Wild, M., Knutti, R., Mishchenko M.I., and Heidinger, A.K.: Consistency of global satellite-derived
582 aerosol and cloud data sets with recent brightening observations, *Geophys. Res. Lett.*, 37, L21704,
583 doi:10.1029/2010GL044632, 2010.
- 584 Chaloulakou, A., Kassomenos, P., Spyrellis, N., Demokritou, P., and Koutrakis, P.: Measurements of PM₁₀ and
585 PM_{2.5} particle concentrations in Athens, Greece, *Atmos. Environ.*, 37, 649 – 660, doi: 10.1016/S1352-
586 2310(02)00898-1, 2003.
- 587 Chan, Y.C., Simpson, R.W., Mctainsh, G.H., Vowles, P.D., Cohen, D.D., and Bailey, G.M.: Source
588 apportionment of visibility degradation problems in Brisbane (Australia) using the multiple linear regression
589 techniques, *Atmos. Environ.*, 33, 3237–3250, doi:10.1016/S1352-2310(99)00091-6, 1999.
- 590 Chang, D., Song, Y., and Liu, B.: Visibility trends in six megacities in China 1973–2007, *Atmos. Res.*, 94, 161–
591 167, doi:10.1016/j.atmosres.2009.05.006, 2009.
- 592 Che, H. Z., Zhang, X. Y., Li, Y., Zou, Z. J., and Qu, J. J.: Horizontal visibility trends in China 1981-2005,
593 *Geophys. Res. Lett.*, 34, L24706, doi:10.1029/2007GL031450, 2007.
- 594 Colbeck, I., Chung, M.C., and Eleftheriadis, K.: Formation and transport of atmospheric aerosol over Athens,
595 Greece, *Water Air Soil Pollut.*, 223-235, doi:10.1023/A:1021335401558, 2002.
- 596 Davis, R. E.: A synoptic climatological analysis of winter visibility trends in the mideastern United States,
597 *Atmos. Environ.*, 25b, 165-175, doi:10.1016/0957-1272(91)90052-G, 1991.
- 598 Dayan, U., and Levy, I.: The Influence of Meteorological Conditions and Atmospheric Circulation Types on
599 PM₁₀ and Visibility in Tel Aviv, *J. Appl. Meteorol.*, 44, 606-619, doi: /10.1175/JAM2232.1, 2005.
- 600 Deng, J.J., Wang, T. J., Jiang, Z.Q., Xie, M., Zhang, R. J., Huang, X. X., and Zhu, J. L.: Characterization of
601 visibility and its affecting factors over Nanjing, China, *Atmos. Res.*, 101, 681–691,
602 doi:10.1016/j.atmosres.2011.04.016, 2011.



- 603 Doyle, M., and Dorling, S.: Visibility trends in the UK 1950-1997, *Atmos. Environ.*, 36, 3161-3172,
604 doi:10.1016/S1352-2310(02)00248-0, 2002.
- 605 Draxler, R., Stunder, B., Rolph, G., Stein, A., and Taylor, A.: Hybrid Single-Particle Lagrangian Integrated
606 Trajectories (HY-SPLIT): Version 4.9 - User's Guide and Model Description,
607 [http://www.arl.noaa.gov/documents/reports/hysplit user guide.pdf](http://www.arl.noaa.gov/documents/reports/hysplit%20user%20guide.pdf), 2009.
- 608 Eidels-Dubovoi, S.: Aerosol impacts on visible light extinction in the atmosphere of Mexico City, *Sci. Total*
609 *Environ.*, 287, 213-220, doi:10.1016/S0048-9697(01)00983-4, 2002.
- 610 Elias, T., Haeffelin, M., Drobinski, P., Gomes, L., Rangognio, J., Bergot, T., Chazette, P., Raut, J.C., and
611 Colomb, M.: Particulate contribution to extinction of visible radiation: pollution, haze, and fog, *Atmos. Res.*, 92,
612 443-454, doi:10.1016/j.atmosres.2009.01.006, 2009.
- 613 Eltbaakh Y. A., Ruslan, M. H., Alghoul, M. A., Othman, M. Y., and Sopian, K.: Issues concerning atmospheric
614 turbidity indices, *Renw. Sustain. Energy Rev.*, 16, 6285-6294, doi: 10.1016/j.rser.2012.05.034, 2012.
- 615 Folini, D., and Wild, M.: Aerosol emissions and dimming/brightening in Europe: Sensitivity studies with
616 ECHAM5-HAM, *J. Geophys. Res.*, 116, D21, doi:10.1029/2011JD016227, 2011.
- 617 Founda, D.: Evolution of the air temperature in Athens and evidence of climatic change: A review, *Advances in*
618 *Building Energy Research*, 5, 7- 41, doi:10.1080/17512549.2011.582338, 2011.
- 619 Founda, D., Pierros, F., Petrakis, M., and Zerefos, C.: Inter-decadal variations and trends of the Urban Heat
620 Island in Athens (Greece) and its response to heat waves, *Atmos. Res.*, 161, 1-13.
621 doi:10.1016/j.atmosres.2015.03.016, 2015.
- 622 Gerasopoulos, E., Kouvarakis, G., Vrekoussis, M., Kanakidou, M., and Mihalopoulos, N.: Ozone variability in
623 the marine boundary layer of the Eastern Mediterranean based on 7-year observations, *J. Geophys. Res.*, 110,
624 D15309, doi:10.1029/2005JD005991, 2005.
- 625 Gerasopoulos, E., Amiridis, V., Kazadzis, S., Kokkalis, P., Eleftheratos, K., Andreae, M. O., Andreae, T. W., El-
626 Askary, H., and Zerefos, C. S.: Three-year ground based measurements of aerosol optical depth over the Eastern
627 Mediterranean: The urban environment of Athens, *Atmos. Chem. Phys.*, 11, 2145-2159, doi:10.5194/acp-11-
628 2145-2011, 2011.
- 629 Ghim, Y.S., Moon, K., Lee, S., and Kim, Y. P.: Visibility trends in Korea during the past two decades, *J. Air*
630 *Waste Manage Assoc.*, 55, 73-82, doi:10.1080/10473289.2005.10464599, 2005.



- 631 Gkikas, A., Basart, S., Hatzianastassiou, N., Marinou, E., Amiridis, V., Kazadzis, S., Pey, J., Querol, X., Jorba,
632 O., Gassó, S., and Baldasano, J. M.: Mediterranean desert dust outbreaks and their vertical structure based on
633 remote sensing data, *Atmos. Chem. Phys.*, 15, 27675-27748, doi:10.5194/acpd-15-27675-2015, 2015.
- 634 Grivas, G., Chaloulakou, A., Samara, C., and Spyrellis, N.: Spatial and temporal variation of PM10 mass
635 concentrations within the Greater Area of Athens, Greece, *Water Air Soil Pollut.*, 158, 357-71,
636 doi:10.1023/B:WATE.0000044859.84066.09, 2004.
- 637 Hamonou, E., Chazette, P., Balis, D., Dulac, F., Schneider, X., Galani, E., Ancellet, G., and Papayannis, A.:
638 Characterization of the vertical structure of Saharan dust export to the Mediterranean basin, *J. Geophys. Res.*, 104,
639 22257-22270, doi:10.1029/1999JD900257, 1999.
- 640 Hand, J.L., Kreidenweis, S.M., Sherman, D. E., Collett, Jr J.L., Hering, S.V., Day, D.E, and Malm, W.C.:
641 Aerosol size distributions and visibility estimates during the Big Bend Regional Aerosol and Visibility
642 Observational (BRAVO) study, *Atmos. Environ.*, 36, 5043-5055, doi:10.1016/S1352-2310(02)00568-X, 2002.
- 643 Hatzianastassiou, N., Gkikas, A., Mihalopoulos, N., Torres, O., and Katsoulis, B. D.: Natural versus
644 anthropogenic aerosols in the eastern Mediterranean basin derived from multiyear TOMS and MODIS satellite
645 data, *J. Geophys. Res.*, 114, D24202, doi:10.1029/2009JD011982, 2009.
- 646 Hoek, G., Forsberg, B., Borowska, M., Hlawiczka, S., Vaskovi, E., Welinder, H., et al.: Wintertime PM 10 and
647 black smoke concentrations across Europe: results from the Peace study, *Atmos. Environ.*, 31, 3609-3622,
648 doi:10.1016/S1352-2310(97)00158-1, 1997.
- 649 Ichoku, C., Chu, D.A., Mattoo, S. et al.: A spatio-temporal approach for global validation and analysis of MODIS
650 aerosol products, *Geophys. Res. Lett.*, 29, 1- 4, doi:10.1029/2001GL013206, 2002.
- 651 Kalabokas, P. D., Viras, L.G., and Repapis, C.C.: Analysis of 11-year record (1987-1997) of air pollution
652 measurements in Athens, Greece, Part I: primary air pollutants, *Global Nest*, 1, 157-167, 1999a.
- 653 Kalabokas, P.D., Viras, L.G., Repapis, C.C., and Bartzis, J.G.: Analysis of 11-year record (1987-1997) of air
654 pollution measurements in Athens, Greece, Part II: photochemical air pollutants, *Global Nest*, 1, 169-176, 1999b.
- 655 Kanakidou, M., Mihalopoulos, N., Kindap, T., Im, U. et al.: Megacities as hot spots of air pollution in the East
656 Mediterranean, *Atmos. Environ.*, 45, 1223-1235, doi:10.1016/j.atmosenv.2010.11.048, 2011.
- 657 Kanellopoulou, E.: Study of the visibility of Athens. PhD Thesis (in Greek), 1979.
- 658 Kim, K. W.: Physico-chemical characteristics of visibility impairment by airborne pollen in an urban area,
659 *Atmos. Environ.*, 41, 3565-357, doi:10.1016/j.atmosenv.2006.12.054, 2007.



- 660 Kim, K.W.: Optical Properties of Size-Resolved Aerosol Chemistry and visibility Variation Observed in the
661 Urban Site of Seoul, Korea, *Aerosol Air Qual. Res.*, 15, 271–283, doi: 10.4209/aaqr.2013.11.0347, 2015.
- 662 Koschmieder, H.: Theorie der horizontalen sichtweite, *Beitr. Phys. Frei. Atmos.*, 12, 171–181, 1924.
- 663 Larson, S.M., and Cass, G.R.: Characteristics of summer midday low-visibility events in the Los Angeles area,
664 *Environ. Sci. Technol.*, 23, 281–289, doi: 10.1021/es00180a003, 1989.
- 665 Lee, D. O.: Regional variations in long-term visibility trends in the UK (1962–1990), *Geog.*, 79, 108–121,
666 <http://www.jstor.org/stable/40572408>, 1994.
- 667 Léon, J.-F., Chazette, P., and Dulac, F.: Retrieval and monitoring of aerosol optical thickness over an urban area
668 by spaceborne and ground-based remote sensing, *Appl. Opt.*, 38, 6918–6926, doi:10.1364/AO.38.006918, 1999
- 669 Lelieveld, J., Berresheim, H., Borrmann, S., Crutzen, P. J., et al.: Global Air Pollution Crossroads over the
670 Mediterranean, *Science*, 298, 794–799, doi: 10.1126/science.1075457, 2002.
- 671 Malm, W. C.: Introduction to Visibility, Air Resources Division, National Park Service, Cooperative Institute for
672 Research in the Atmosphere (CIARA), NPS Visibility Program, Colorado State University, Fort Collins, CO, May,
673 1999.
- 674 Maloutas, T.: The self promoting housing solution in post war Athens, Discussion Paper Series 9(6) 95–110,
675 Available online at: http://www.prd.uth.gr/research/DP/2003/uth-prd-dp-2003-6_en.pdf, 2003.
- 676 Mavroidis, I., and Iliá, M.: Trends of NOX, NO2 and O3 concentrations, at three different types of air quality
677 monitoring stations in Athens, Greece, *Atmos. Environ.*, 63, 135–147, doi:10.1016/j.atmosenv.2012.09.030, 2012.
- 678 Mylona, S.: Sulfur dioxide emissions in Europe 1880–1991 and their effect on sulphur concentrations and
679 depositions, *Tellus*, 48, 662–689, doi/10.1034/j.1600-0889.1996.t01-2-00005.x, 1996.
- 680 Nabat, P., Somot, S., Mallet, M., Sanchez-Lorenzo, A., and Wild, M.: Contribution of anthropogenic sulfate
681 aerosols to the changing Euro-Mediterranean climate since 1980, *Geophys. Res. Lett.*, 41, 5605–5611,
682 doi:10.1002/2014GL060798, 2014.
- 683 Paraskevopoulou, D., Liakakou, E., Gerasopoulos, E., Theodosi, C., and Mihalopoulos, N.: Long-term
684 characterization of organic and elemental carbon in the PM_{2.5} fraction: the case of Athens, Greece, *Atmos. Chem.*
685 *Phys.*, 14, 13313–13325, doi:10.5194/acp-14-13313-2014, 2014.
- 686 Paraskevopoulou, D., Liakakou, E., Gerasopoulos, E., and Mihalopoulos, N.: Sources of atmospheric aerosol
687 from long-term measurements (5 years) of chemical composition in Athens, Greece, *Sci. Total Environ.*, 527–
688 528, 165–178, doi:10.1016/j.scitotenv.2015.04.022, 2015.



- 689 Remoudaki, E., Gergametti, G., and Losno, R.: On the dynamic of the atmospheric input of copper and
690 manganese into the western Mediterranean Sea, *Atmos. Environ.*, 25A, 733-744, doi:10.1016/0960-
691 1686(91)90072-F, 1991a.
- 692 Remoudaki, E., Gergametti, G., and Buat-Ménard, P.: Temporal variability of atmospheric lead concentrations
693 and fluxes over the northwestern Mediterranean Sea, *J. Geophys. Res.*, 96, 1043-1055, doi:10.1029/90JD00111,
694 1991b.
- 695 Santamouris, M., Paravantis, J.A., Founda, D., Kolokotsa, D., Michalakakou, P., Papadopoulos, A. M.,
696 Kontoulis, N., Tzavali, A., Stigka, E. K., Ioannidis, Z., Mehilli, A., Matthiessen, A., and Servou, E.: Financial
697 Crisis and Energy Consumption: A household Survey in Greece, *Energy Build.*, 65, 477-487,
698 doi:10.1016/j.enbuild.2013.06.024, 2013.
- 699 Singh, A., and Dey, S.: Influence of aerosol composition on visibility in megacity Delhi, *Atmos. Environ.*, 62,
700 367- 373, doi:10.1016/j.atmosenv.2012.08.048, 2012.
- 701 Sloane, C.S.: Visibility trends - I. Mideastern United States 1948-1978, *Atmos. Environ.*, 16, 2309-2321,
702 doi:10.1016/0004-6981(82)90117-2, 1982.
- 703 Stjern, C. W., Stohl, A., and Kristjánsson, J. E.: Have aerosols affected trends in visibility and precipitation in
704 Europe? *J. Geophys. Res.*, 116, D02212, doi:10.1029/2010JD014603, 2011.
- 705 Streets, D. G., Wu, Y., and Chin, M.: Two-decadal aerosol trends as a likely explanation of the
706 globaldimming/brightening transition, *Geophys. Res. Lett.*, 33, L15806, doi:10.1029/2006GL026471, 2006.
- 707 Tang, I.N.: Chemical and size effects of hygroscopic aerosols on light scattering coefficients, *J. Geophys. Res.*,
708 101, 19245–19250, doi: 10.1029/96JD03003, 1996.
- 709 Theodosi, C., Grivas, G., Zarmas, P., Chaloulakou, A., and Mihalopoulos, N.: Mass and chemical composition
710 of size- segregated aerosols (PM₁, PM_{2.5}, PM₁₀) over Athens, Greece: local versus regional sources, *Atmos.*
711 *Chem. Phys.*, 11, 11895– 11911, doi:10.5194/acp-11-11895-2011, 2011.
- 712 Tsai, Y. I, Lin, Y.H., and Lee, S. Z.: Visibility variation with air qualities in the metropolitan area of southern
713 Taiwan, *Water Air Soil Pollut.*, 144, 19-40, doi:10.1023/A:1022901808656, 2003.
- 714 Tsai, Y.I., Kuo, S.C., Lee, W.J., Chen, C.L., and Chen, P.T.: Long-term visibility trends in one highly urbanized,
715 one highly industrialized, and two rural areas of Taiwan, *Sci. Total Environ.*, 382, 324–341,
716 doi:10.1016/j.scitotenv.2007.04.048, 2007.



- 717 van Aardenne, J. A., Dentener, F. J., Olivier, J. G. J., Klein Goldewijk, C. G. M., and Lelieveld, J.: A $1^\circ \times 1^\circ$
718 resolution data set of historical anthropogenic trace gas emissions for the period 1890–1990, *Glob. Biochem.*
719 *Cycles*, 15, 909-928, doi: 10.1029/2000GB001265, 2001.
- 720 van Beelen, A.J., and van Delden, A.J.: Cleaner air brings better views, more sunshine and warmer summer days
721 in the Netherlands, *Weather*, 67, 21-25, doi: 10.1002/wea.854, 2012.
- 722 Vautard, R., Yiou, P., and Oldenborgh, G.: Decline of fog, mist and haze in Europe over the past 30 years, *Nat.*
723 *Geosci.*, 2, 115-119, doi:10.1038/NGEO414, doi:10.1038/ngeo414, 2009.
- 724 Vrekoussis, M., Richter, A., Hilboll, A., Burrows, J. P., Gerasopoulos, E., Lelieveld, J., Barrie, L., Zerefos, C.,
725 and Mihalopoulos, N.: Economic crisis detected from space: Air quality observations over Athens, Greece,
726 *Geophys. Res. Lett.*, 40, 458-463, doi:10.1002/grl.50118, 2013.
- 727 Wan, J.M., Lin, M., Chan, C.Y., Zhang, Z.S., Engling, G., Wang, X.M., Chan, I.N., and Li, S.Y.: Change of air
728 quality and its impact on atmospheric visibility in central-western Pearl River Delta, *Environ. Monit. Assess.*,
729 172, 339-351, doi: 10.1007/s10661-010-1338-2, 2011.
- 730 Wang, K., Dickinson, R.E., and Liang, S.: Clear sky visibility has decreased over land globally from 1973 to
731 2007, *Science*, 323, 1468-1470, doi:10.1126/science.1167549, 2009.
- 732 Wang, K. C., Dickinson, R. E., Su, L., and Trenberth, K. E.: Contrasting trends of mass and optical properties of
733 aerosols over the Northern Hemisphere from 1992 to 2011, *Atmos. Chem. Phys.*, 12, 9387–9398,
734 doi:10.5194/acp-12-9387-2012, 2012.
- 735 Wild, M., 2009: Global dimming and brightening: A review, *J. Geophys. Res.*, 114, doi: 10.1029/2008JD011470,
736 2009.
- 737 Wu, J., Fu, C., Zhang, L., and Tang, J.: Trends of visibility on sunny days in China in the recent 50 years, *Atmos.*
738 *Environ.*, 5, 339-346, doi:10.1016/j.atmosenv.2012.03.037, 2012.
- 739 World Meteorological Organization: The WMO Automatic Digital Barometer inter comparison (J. P. van der
740 Meulen), Instrument and Observing Methods Report No.46, WMO/TD-No.474, Geneva, 1992.
- 741 Zhao, P., Zhang, X., Xu, X. and Zhao, X.: Long-Term Visibility Trends and Characteristics in the Region of
742 Beijing, Tianjin, and Hebei, China, *Atmos. Res.*, 101, 711–718, doi:10.1016/j.atmosres.2011.04.019, 2011.
- 743



744

745 Table 1: Mean monthly and yearly values with standard deviations of basic climatic elements in Athens (NOA),
 746 calculated from the WMO climatic period (1971-2000). (**)

Month	Tmean (°C)	Tmax (°C)	Tmin (°C)	RH (%)	Rainfall (mm)	Number of rainy days (> 1 mm)	Wind Speed (m s ⁻¹)
January	9.3 ± 1.1	13.0 ± 1.3	6.6 ± 1.1	72.1 ± 3.9	42.5 ± 31	5.6 ± 3.0	3.1 ± 0.71
February	9.6 ± 1.4	13.7 ± 1.7	6.8 ± 1.4	70.2 ± 3.5	44.8 ± 29	5.6 ± 2.1	3.4 ± 0.50
March	11.5 ± 1.4	16.1 ± 1.8	8.2 ± 1.3	67.6 ± 4.3	50.2 ± 41	5.4 ± 2.6	3.3 ± 0.72
April	15.4 ± 1.3	20.5 ± 1.6	11.5 ± 1.1	62.7 ± 4.6	32.7 ± 29	4.2 ± 2.6	2.8 ± 0.51
May	20.3 ± 1.1	25.7 ± 1.3	16.1 ± 1.1	57.3 ± 4.0	16.7 ± 16	2.6 ± 1.9	2.9 ± 0.45
June	25.0 ± 0.9	30.6 ± 1.2	20.4 ± 0.9	51.3 ± 3.7	7.5 ± 10	0.9 ± 1.0	3.1 ± 0.60
July	27.3 ± 1.1	33.1 ± 1.4	22.7 ± 1.1	48.5 ± 4.2	6.6 ± 9	0.9 ± 1.1	3.5 ± 0.75
August	26.8 ± 1.2	33.7 ± 1.4	22.5 ± 1.2	49.8 ± 5.1	7.2 ± 12	0.9 ± 1.2	3.5 ± 0.58
September	23.4 ± 1.1	29.2 ± 1.5	19.4 ± 1.0	57.0 ± 4.7	9.4 ± 1	1.3 ± 1.6	2.9 ± 0.47
October	18.5 ± 1.5	23.5 ± 1.8	15.1 ± 1.6	66.4 ± 3.7	42.9 ± 40	3.7 ± 2.4	2.9 ± 0.74
November	14.0 ± 1.3	18.1 ± 1.5	11.1 ± 1.3	72.7 ± 3.8	59.9 ± 45	7.9 ± 3.8	2.9 ± 0.73
December	10.8 ± 1.4	14.4 ± 1.8	8.2 ± 1.3	74.0 ± 3.2	62.6 ± 34	9.0 ± 13.4	3.0 ± 0.56
Year	17.7 ± 0.5	22.6 ± 0.7	14.1 ± 0.5	62.0 ± 1.9	389.5 ± 5	42.9 ± 9.0	3.1 ± 0.36

747

748

749

750

751

(**) Climatic means were calculated from daily observations at NOA over the period 1971-2000. Daily time series are almost complete, with sporadic missing data in certain variables. In particular, data availability for the period 1971-2000 equals 100 % for Tmax, Tmin and rainfall, 99.9 % for Tmean, 99.8 % for RH and 99.4% for the wind speed.



752

753

754 Table 2: The WMO empirical scale for visibility observations, used at NOAA.

Visibility Classes	1	2	3	4	5	6	7	8	9
Visibility Ranges	50- 200m	200- 500m	500- 1000m	1-2 km	2-4 km	4-10 km	10-20 km	20-50 km	>50km

755

756

757

758

759

760

761

762

763

764

765

766

767

768

769

770

771



Fig.1. Map of the study area in Greece, including the Athens urban station (NOA) and a reference, non-urban station (HER) at Heraklion airport, Crete. The gray surface represents the boundary of the Greater Athens Area (GAA).



796

797

798

799

800

801

802

803

804

805

806

807



808

Fig. 2a. Main sectors related with air masses origin in Athens.

809

810

811

812

813

814

815

816

817

818

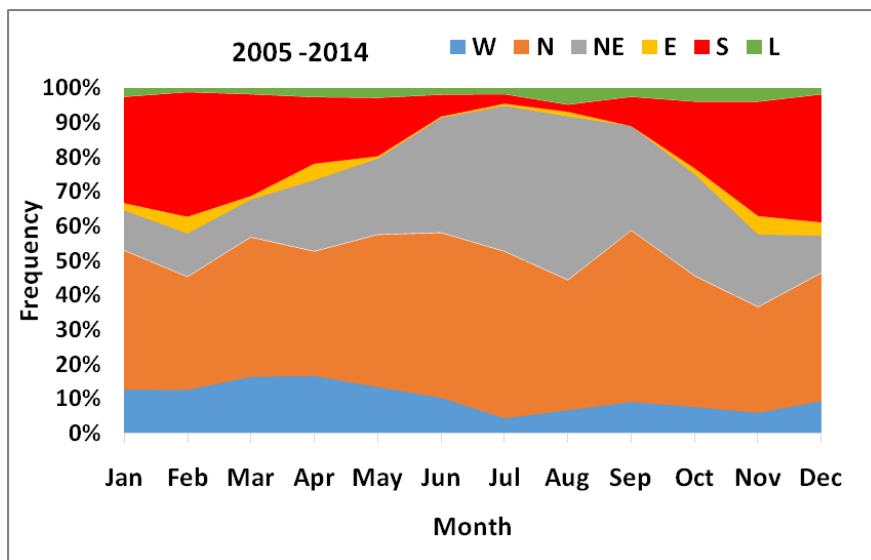


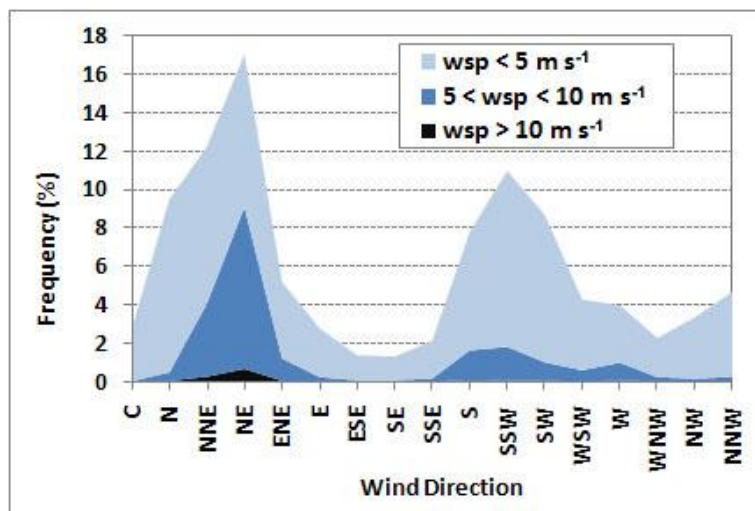
Fig. 2b. Seasonal variability of the relative frequency of air masses origin in Athens on the sectors defined in Fig. 2a, averaged over the period 2005-2014. Category 'L' refers to air masses of local origin.



843

844

845



846

847 **Fig. 3.** Frequencies of surface wind directions for three wind speed (wsp) categories at NOA, based on hourly
848 values of the period 1971-2000. For instance, the NE direction occurs cumulatively at a frequency of 17% which
849 is the sum of 7.9 % ($wsp < 5 \text{ m s}^{-1}$), 8.4 % ($5 < wsp < 10 \text{ m s}^{-1}$) and 0.7 % ($wsp > 10 \text{ m s}^{-1}$). The 'C' sector
850 corresponds to calms ($wsp < 0.3 \text{ m s}^{-1}$).

851

852

853

854

855

856

857

858

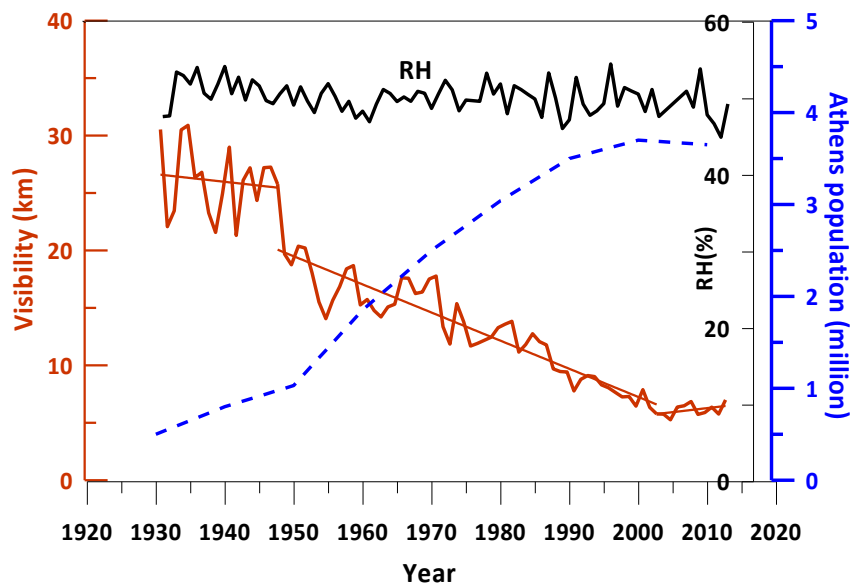
859



860

861

862



863

864 **Fig. 4.** Inter-decadal variability of the annual visibility in Athens from 1931 to 2013, along with linear trends for
865 three sub-periods: 1931-1948, 1949-2003 and 2004-2013 (red line). The dashed blue line presents the population
866 growth in Athens (in millions) since 1930 (Founda, 2011). The long-term variability of the annual relative
867 humidity (RH) in Athens is also displayed (upper black line).

868

869

870

871

872

873

874

875



876

877

878

879

880

881

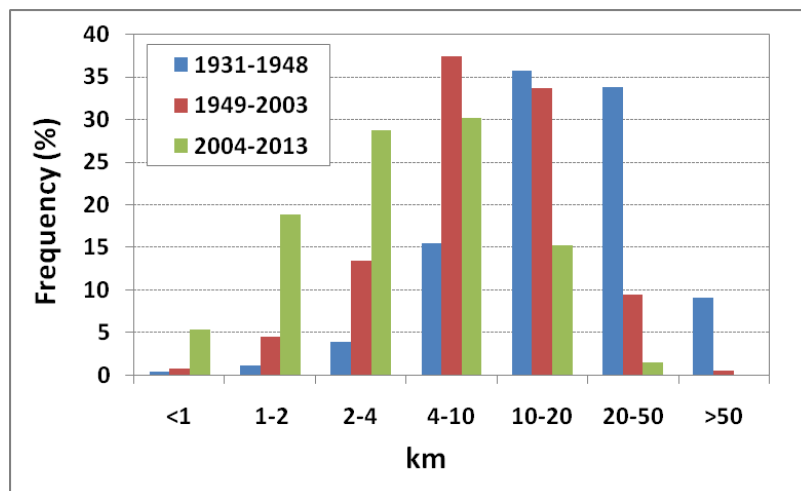
882

883

884

885

886



887 **Fig. 5.** Frequency distribution of different visibility ranges (Table 2) in Athens for the three sub-periods, 1931-
888 1948, 1949-2003 and 2004-2013.

889

890

891

892

893

894

895

896

897

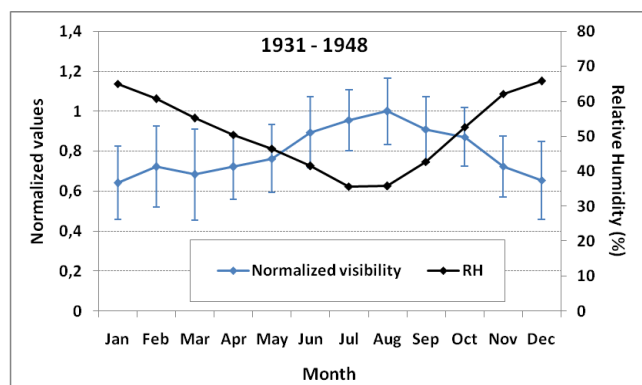
898



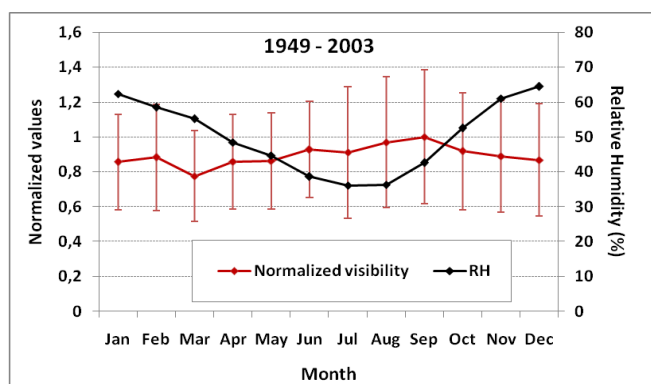
899

900

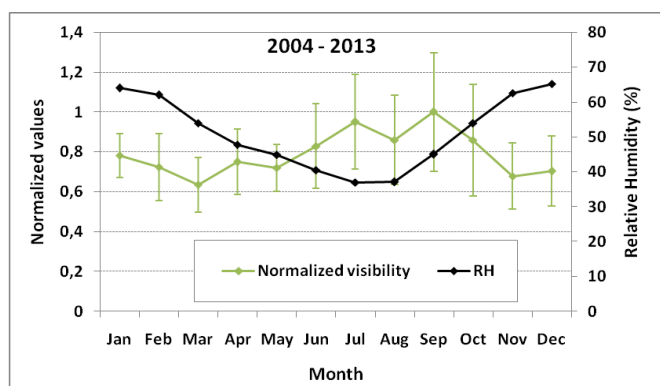
901



902



903



904 **Fig. 6.** Normalized mean monthly values of visibility in Athens for the three sub-periods, along with mean
905 monthly values of relative humidity (RH) for each sub-period. Vertical lines represent standard deviations of
906 mean monthly values of visibility.

907

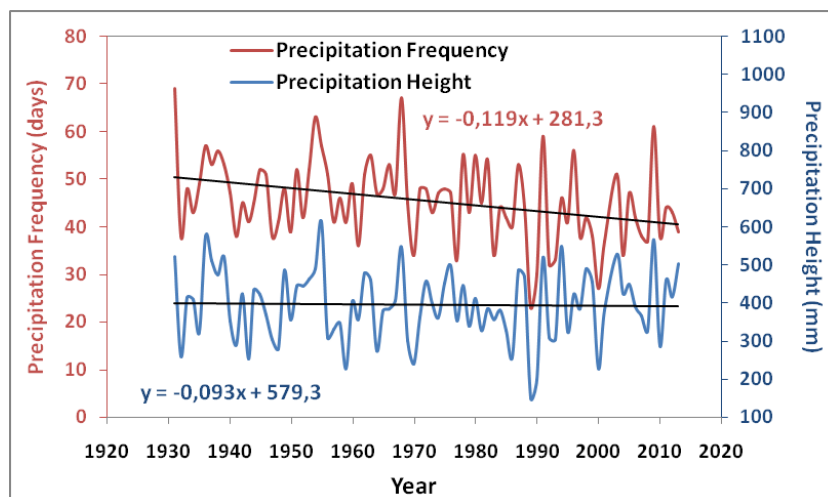


Fig. 7. Variation and long-term linear trends of the annual precipitation amount and frequency (number of days per year with precipitation > 1 mm) at NOAA, over the period 1931-2013. Slopes of linear trends are also shown.

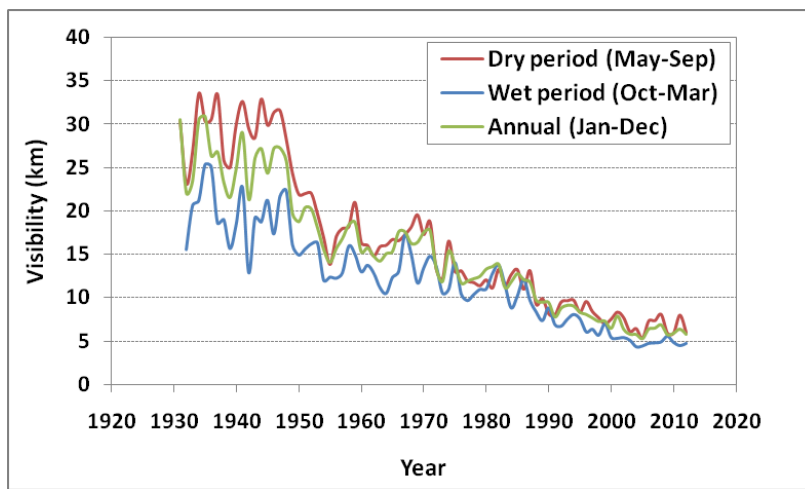


Fig. 8. Variation of visibility at NOA from 1931-2013 during the dry (May-Sep.), wet (Oct.-Mar.) and all year (Jan.-Dec.) period.

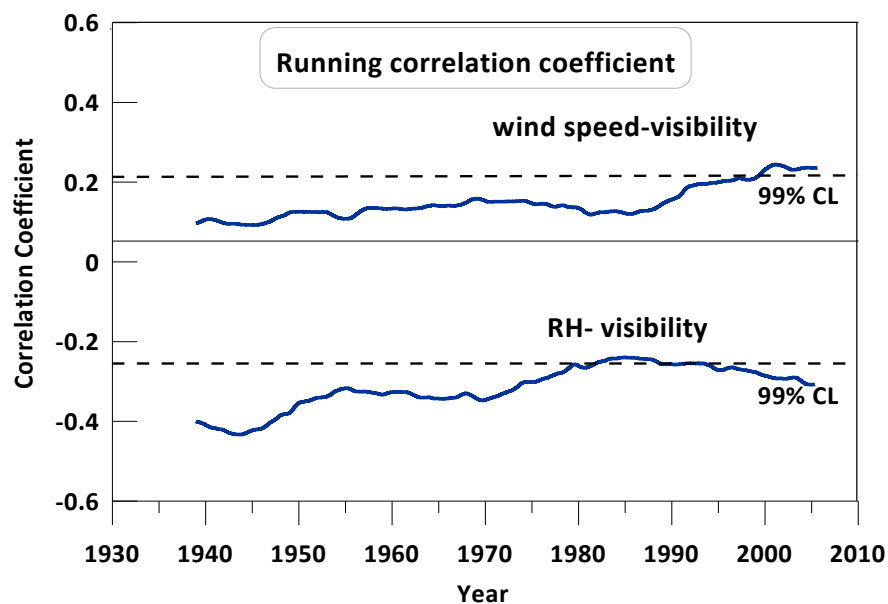


Fig. 9. Running correlation coefficient and confidence levels between visibility and wind speed (up) and visibility and RH (bottom) in Athens, over the period 1931-2013. A 15-yrs window was used.

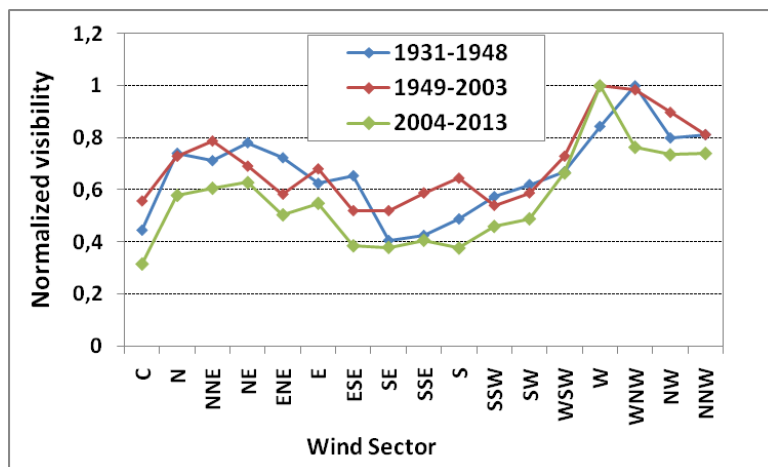


Fig. 10. Variation of visibility with wind direction (sectors) over the three sub-periods 1931-1948, 1949-2003 and 2004-2013. Visibility is normalized by its maximum value at a certain sector for each sub-period. Sector ‘C’ corresponds to calms (wind speed $< 0.3 \text{ m s}^{-1}$). Frequency of each sector approximates closely its climatic value (Fig. 3) in all sub-periods.

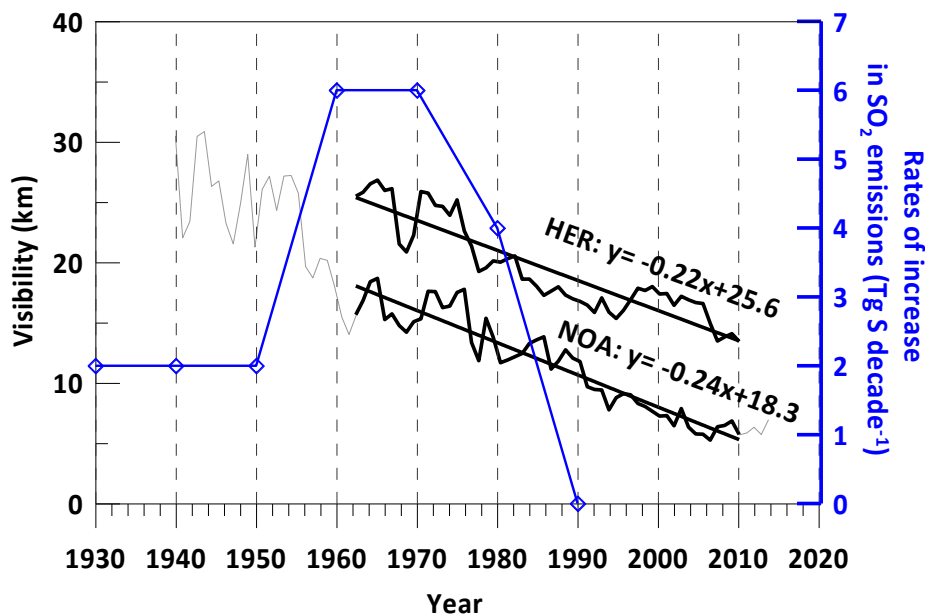
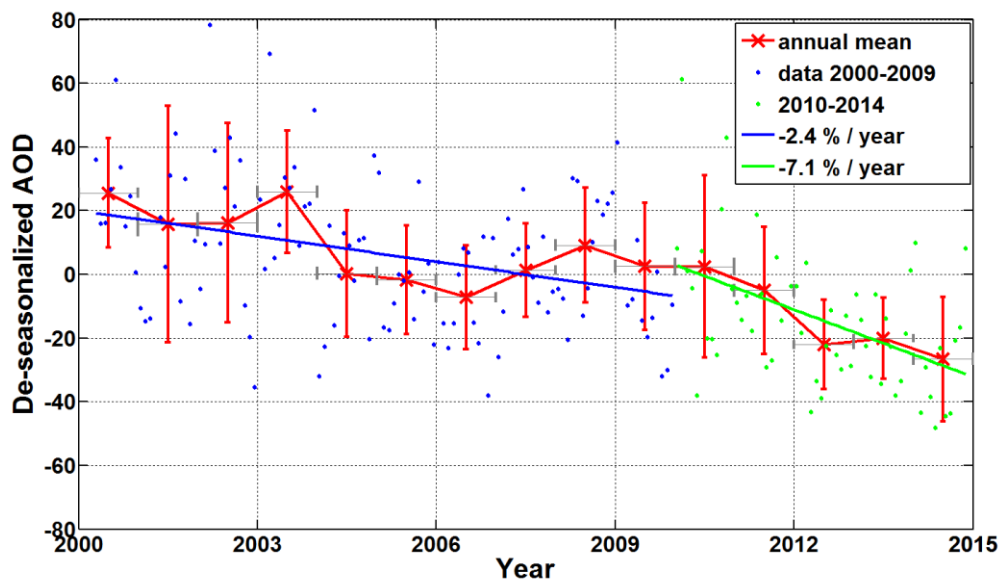


Fig. 11. Inter-decadal variability of the annual visibility at NOA (urban) and HER (background) stations. Bold black lines represent the common period of observations (1956-2009) at the two stations along with linear trends and slopes. Blue line illustrates the rates of increase of SO₂ emissions in Europe (in Tg S decade⁻¹), as included in van Aardenne et al., 2001.



1018
1019
1020



1021
1022
1023
1024
1025
1026
1027
1028
1029
1030
1031
1032
1033

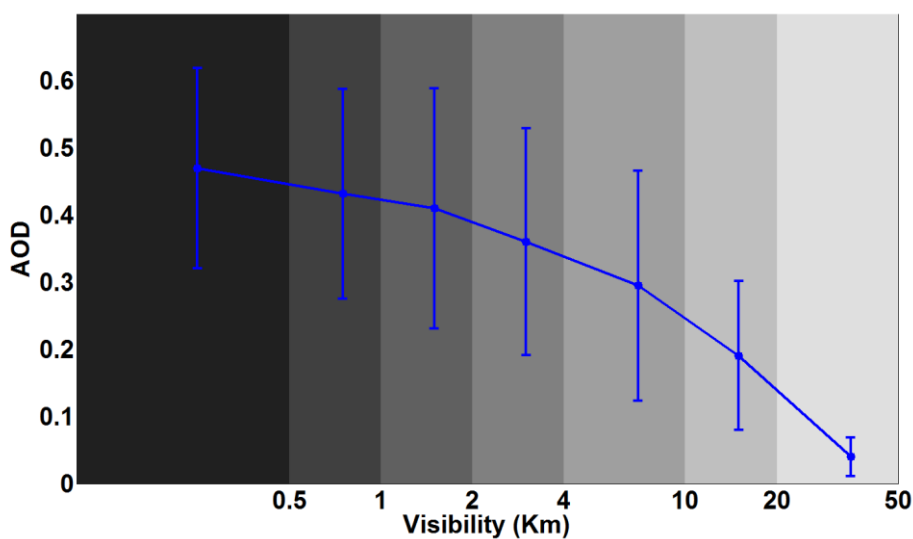
Fig. 12. Variability of deseasonalized monthly AOD_{550nm} from 2000 to 2014 (red), along with linear trends for the periods 2000-2009 (blue), 2010-2014 (green). Vertical bars describe the standard deviation of the annual value based on the monthly ones and grey horizontal bars the respective year.



1034

1035

1036



1037

1038 **Fig. 13.** MODIS AOD June-August mean values and standard deviations for each visibility index. Shaded areas
1039 represent visibility ranges (km) for each visibility class (Table 2) and points are plotted at the center of each
1040 visibility class.

1041

1042

1043

1044

1045

1046

1047

1048

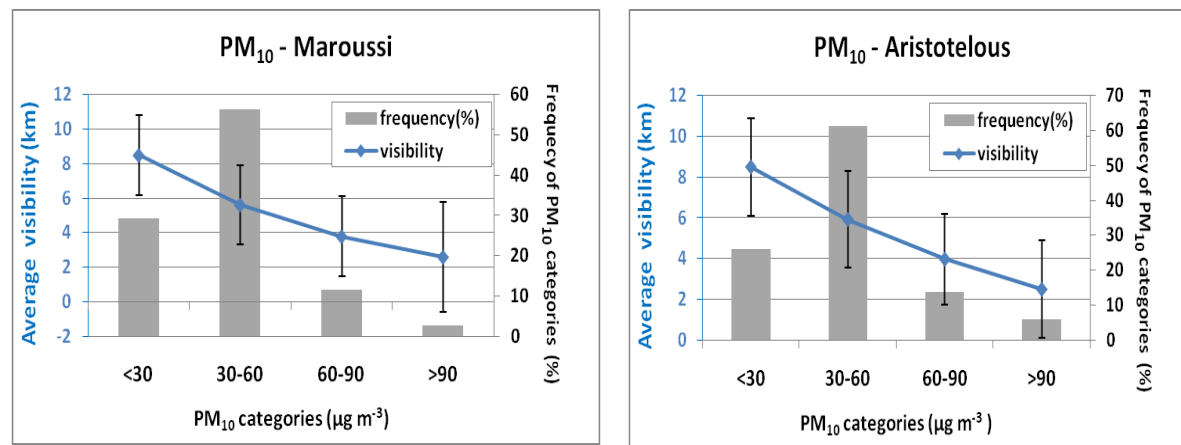
1049



1050

1051

1052



1053

1054 **Fig. 14.** Visibility as a function of different classes of PM₁₀ levels at an urban (Aristotelous) and a suburban
1055 (Maroussi) station in Athens. Measurements refer to the period 2008-2012. Geometric average and geometric
1056 standard deviations are applied on visibility observations. Frequencies of classes of PM₁₀ levels are also shown
1057 (grey bars).

1058

1059

1060

1061

1062

1063

1064

1065

1066

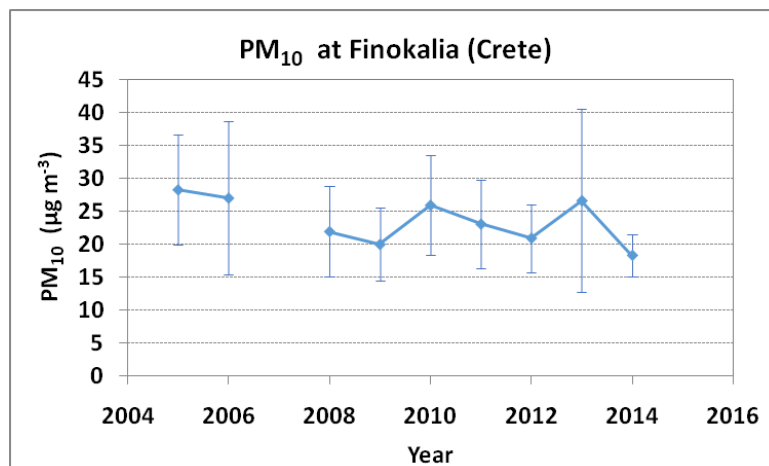


Fig. 15. Variation of the annual PM₁₀ concentrations at the reference station of Finokalia (Crete) over the period 2005-2014. Vertical lines represent standard deviations of the annual means.